

# Continuum model for dislocation structures of semicoherent interfaces

Luchan Zhang, Xiaoxue Qin, Yang Xiang\*

*Department of Mathematics, Hong Kong University of Science and Technology, Clear Water Bay, Kowloon, Hong Kong*

---

## Abstract

In order to relieve the misfitting elastic energy, the hetero-interfaces become semicoherent by forming networks of dislocations. These microscopic structures strongly influence the materials properties associated with the development of advanced materials. We develop a continuum model for the dislocation structures of semicoherent interfaces. The classical Frank-Bilby equation that governs the dislocation structures on semicoherent interfaces is not able to determine a unique solution. The available methods in the literature either use further information from atomistic simulations or consider only special cases (dislocations with no more than two Burgers vectors) where the Frank-Bilby equation has a unique solution. In our continuum model, the dislocation structure of a semicoherent interface is obtained by minimizing the energy of the equilibrium dislocation network with respect to all the possible Burgers vectors, subject to the constraint of the Frank-Bilby equation. The continuum model is validated by comparisons with atomistic simulation results.

*Keywords:* Semicoherent interfaces, Dislocations, Frank-Bilby equation, Energy minimization

---

## 1. Introduction

The interfaces between different materials or different phases commonly form semicoherent structures that consist of discrete dislocation networks to accommodate the lattice misfit

---

\*Corresponding author

*Email address:* maxiang@ust.hk (Yang Xiang)

between the two materials [1, 2, 3]. Such semicoherent interfaces play essential roles in the mechanical, electronic and plasticity properties that are associated with the development of novel composite materials and alloys [1, 2, 3, 4, 5, 6, 7, 8, 9, 10, 11, 12, 13, 14, 15]. These properties strongly depend on the characteristics of the dislocation networks of the semicoherent interfaces.

A semicoherent interface is composed of a network of misfitting dislocations and coherent regions separated by these dislocations. The equilibrium dislocation structure on a semicoherent interface is governed by the Frank-Bilby equation [16, 17], which determines the net Burgers vector content  $\mathbf{B}(\mathbf{p})$  crossing a probe vector  $\mathbf{p}$  on the interface. The Frank-Bilby equation strongly depends on the reference state and the possible Burgers vectors defined associated with it, on which there have been some in-depth discussions in the literature, e.g., [6, 7, 8, 9, 10, 11, 12, 13].

However, even though the reference state and all the associated possible Burgers vectors on a semicoherent interface are determined, the Frank-Bilby equation is still not able to give a unique dislocation structure. See the example discussed at the end of Sec. 2. Wang *et al.* [7, 9] have developed an atomically informed Frank-Bilby theory by combining the classical Frank-Bilby theory and atomistic simulations to determine the reference lattice and interfacial dislocation structure of a heterogeneous interface. The dislocation line directions and their Burgers vectors in the dislocation structure in the Frank-Bilby equation are informed by atomistic simulation results. Vattre and Demkowicz, Abdolrahim and Demkowicz [8, 10, 11] have formulated approaches to determine the reference state for the interfacial misfitting dislocation arrays, linking the Frank–Bilby equation and anisotropic elasticity theory under the condition of vanishing far-field stresses. They considered two sets of misfitting dislocations (i.e., dislocations with two possible Burgers vectors) in their theory, for which the Frank–Bilby equation is able to give a unique solution. Generalization of this approach has been proposed by Vattre [12] to incorporate hexagonal misfitting dislocation networks with new dislocation segments with the third Burgers vector formed by dislocation reaction, from the lozenge dislocation network of two sets of dislocations solved using the method in Ref. [8, 10]. Further generalizations have been made by Vattre and Pan [13] for

interaction and movements of various dislocations in anisotropic bicrystals with semicoherent interfaces. There are also simulations for the dislocation/disconnection structures on semicoherent interfaces of precipitates with prescribed Burgers vectors [4, 5].

In this paper, we present a continuum model to obtain the dislocation structure of a semicoherent interface, given the reference state and all possible Burgers vectors. In the continuum model, the energy of the equilibrium misfitting dislocation network is minimized with respect to all possible Burgers vectors subject to the constraint of the Frank-Bilby equation. The continuum model is based on the orientation-dependent dislocation densities of the dislocation structure. Since the Frank-Bilby equation holds, the long-range elastic energy vanishes, and the energy of the heterogeneous interface consists of only the local energy of the equilibrium dislocation network, for which the continuum formulation for the local energy of dislocation arrays [18] is used. When the dislocation network consists of straight dislocations, our continuum model gives the exact solution (i.e., exact dislocation line directions and inter-dislocation distances) of the dislocation network. We also develop an identification method based on dislocation reactions to recover the exact dislocation network (e.g., the hexagonal network) from the orientation-dependent dislocation densities obtained in the continuum model. This model is a generalization of the method proposed in Ref. [19] for finding dislocation structures of low angle grain boundaries.

Numerically, the constrained minimization problem in our continuum model is solved by the penalty method. We use our continuum model to study the fcc/bcc semicoherent interfaces with the Nishiyama-Wassermann (NW) and Kurdjumov-Sachs (KS) orientation relations. Comparisons with atomistic simulations show that our continuum model can provide excellent predictions of the dislocation structures of semicoherent interfaces.

This paper is organized as follows. In Sec. 2, we review the semicoherent interfaces and the Frank-Bilby equation. In Sec. 3, we present our continuum model for the dislocation structure. The reference lattices and possible Burgers vectors of some semicoherent interfaces are reviewed in Sec. 4. In Sec. 5, we apply our continuum model to obtain the dislocation structures of Cu/Nb semicoherent interfaces, and compare the results with those of atomistic simulations in Ref. [7, 9]. Conclusion and discussion are made in Sec. 6.

## 2. Semicoherent interfaces and Frank-Bilby equation

We first review the semicoherent interfaces and the Frank-Bilby equation. The geometry of a bicrystal hetero-interface is illustrated schematically in Fig. 1(a). Two materials (or two phases)  $\alpha$  and  $\beta$  with different lattice structures are joined, and a hetero-interface is formed between them. The interface plane is set as the  $xy$  plane. When the lattice structures of the adjacent crystals are similar, and the lattice spacing difference between the unstrained adjacent crystals are relatively small, the interface usually becomes semicoherent by forming a network of misfit dislocations on the interface, and atoms in two adjacent lattices are adjusted by additional strains or rotations. Figure 1(b) demonstrates a natural dichromatic pattern of the semicoherent interface between fcc(110)/bcc(001).

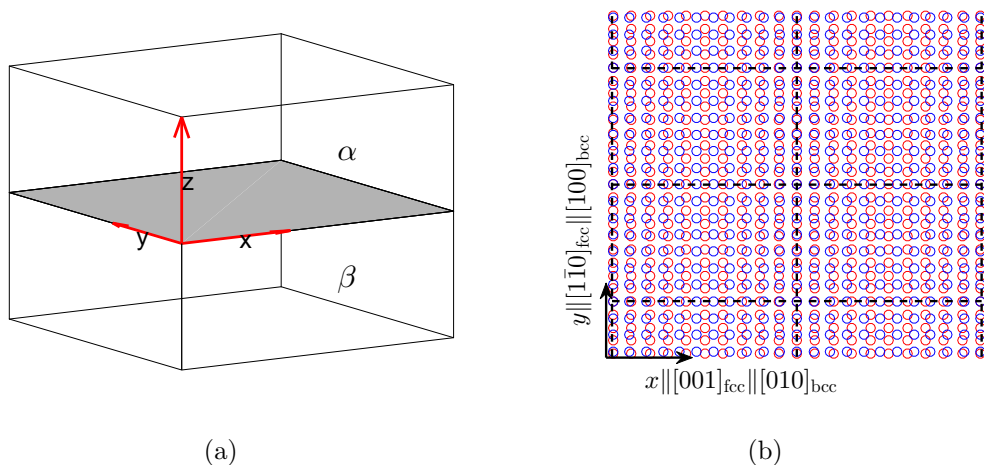


Figure 1: (a) Illustration of the bicrystal hetero-interface. (b) The natural dichromatic pattern of the interface between fcc(110)/bcc(001).

Frank and Bilby proposed a theory that provides an geometry constraint of the equilibrium dislocation structure on a semicoherent interface [16, 17]. Given the reference lattice, the Frank-Bilby theory determines the net Burgers vector  $\mathbf{B}(\mathbf{p})$  crossing an interfacial probe vector  $\mathbf{p}$  as  $\mathbf{B}(\mathbf{p}) = (\mathbf{S}_\beta^{-1} - \mathbf{S}_\alpha^{-1})\mathbf{p}$ , where  $\mathbf{S}_\alpha^{-1}, \mathbf{S}_\beta^{-1}$  respectively are inverse matrices of the distortion transformation matrices  $\mathbf{S}_\alpha, \mathbf{S}_\beta$  that map the lattice vectors from the natural unstrained lattices  $\alpha, \beta$  to the reference lattice.

Once the reference lattice is determined, there will be finite number of possible Burgers vectors associated with it, which are the lattice vectors in the reference lattice. We denote these Burgers vectors by  $\mathbf{b}_j$ ,  $j = 1, 2, \dots, J$ . The net Burgers vector  $\mathbf{B}(\mathbf{p})$  can be expressed in the reference lattice as  $\mathbf{B}(\mathbf{p}) = \sum_{j=1}^J (\mathbf{N}_j \cdot \mathbf{p}) \mathbf{b}_j$ . Recall that in the classical dislocation model of grain boundaries and interfaces [3, 20], the dislocation structure on a boundary/interface is described by the reciprocal vector  $\mathbf{N}$  lying in the boundary/interface plane that is perpendicular to the dislocation and has magnitude  $N = 1/D$ , where  $D$  is the inter-dislocation distance. The local dislocation line direction is  $\boldsymbol{\xi} = (\mathbf{N}/N) \times \mathbf{n}$ , where  $\mathbf{n}$  is the unit normal vector of the interface (which is in the  $+z$  direction here). The dislocation density is  $N$ . For multiple arrays of dislocations on the interface, the dislocation array with Burgers vectors  $\mathbf{b}_j$  are represented by  $\mathbf{N}_j$ ,  $j = 1, 2, \dots, J$ . Accordingly, the **Frank-Bilby equation** can be written as

$$\sum_{j=1}^J (\mathbf{N}_j \cdot \mathbf{p}) \mathbf{b}_j = (\mathbf{S}_\beta^{-1} - \mathbf{S}_\alpha^{-1}) \mathbf{p}, \quad (1)$$

for any interfacial probe vector  $\mathbf{p}$ .

The Frank-Bilby equation in general is not able to uniquely determine the dislocation structure. For example, on the fcc(110)/bcc(001) interface with  $[001]_{\text{fcc}} \parallel [010]_{\text{bcc}}$  and  $[\bar{1}\bar{1}0]_{\text{fcc}} \parallel [100]_{\text{bcc}}$ , there are four possible Burgers vectors [7], leading to 8 unknowns of the four vectors  $\mathbf{N}_j = (N_{jx}, N_{jy})$  for the orientations and inter-dislocation distances of the four sets of Burgers vectors; whereas there are only 4 equations in Frank-Bilby theory, which are not enough to determine the 8 unknown quantities. Only when there are no more than two possible Burgers vectors in the semicoherent interface, the Frank-Bilby equation can uniquely determine a dislocation structure.

Our continuum model will be based on the given reference state. In this paper, we simply adopt the median lattice (average of the two lattices) with isotropic elasticity. In practice, the median lattice or one of the adjacent lattices have often been used as the reference lattice [16, 21, 3]. Especially, the median lattice [16] is an excellent approximation of the reference lattice for symmetric and isotropic interfaces, leading to equal partition of the elastic fields of the two crystals. Recently, methods of determining the reference lattice in general cases

such as anisotropic or unsymmetrical interfaces have also been developed [6, 7, 8, 9, 10, 11].

The reference lattices and possible Burgers vectors of some hetero-interfaces will be reviewed in Sec. 4.

### 3. Continuum model

Now we present a continuum model to obtain the dislocation structure of the semicoherent hetero-interface with the given reference state (or equivalently, the distortion transformation matrices  $\mathbf{S}_\alpha$  and  $\mathbf{S}_\beta$ ) and all possible Burgers vectors ( $\mathbf{b}_j, j = 1, 2, \dots, J$ ). Since Frank-Bilby equation is not sufficient to uniquely determined the dislocation structure on the interface, we identify the equilibrium dislocation structure by minimizing the local energy associated with the constituent dislocations of the interface subject to the constraint of the Frank-Bilby equation. That is, we solve the following **constrained energy minimization problem** for the dislocation structure:

$$\text{minimize} \quad E = \int_S \gamma dS, \quad (2)$$

$$\text{with} \quad \gamma = \sum_{j=1}^J \frac{\mu b_j^2}{4\pi(1-\nu)} \left( 1 - \nu \frac{(\mathbf{N}_j \times \mathbf{n} \cdot \mathbf{b}_j)^2}{b_j^2 N_j^2} \right) N_j \log \frac{1}{r_g \sqrt{N_j^2 + \epsilon}}, \quad (3)$$

$$\text{subject to} \quad \mathbf{h} = \sum_{j=1}^J (\mathbf{N}_j \cdot \mathbf{p}) \mathbf{b}_j - (\mathbf{S}_\beta^{-1} - \mathbf{S}_\alpha^{-1}) \mathbf{p} = \mathbf{0}. \quad (4)$$

Here  $S$  is a periodic cell on the interface plane,  $\gamma$  is the interface energy density,  $\mu$  is the shear modulus,  $\nu$  is the Poisson ratio,  $b_j$  is the length of the  $j$ -th Burgers vector,  $r_g$  is a parameter associated with the dislocation core size,  $\epsilon$  is some small positive regularization parameter to avoid the numerical singularity when  $N_j = 0$ . The constraint in Eq. (4) is the Frank-Bilby equation, which holds for any vector  $\mathbf{p}$  on the interface.

The interface energy  $\gamma$  in Eq. (3) is based on the local energy of dislocation arrays in terms of dislocation densities [18]. Since Frank-Bilby equation is equivalent to cancellation of the long-range elastic field [16, 17, 20, 3], there is only local energy of the constituent dislocations on the interface when Frank-Bilby equation in Eq. (4) holds, as that for the grain

boundaries in homogeneous materials [20, 3]. The elastic constants in  $\gamma$  in Eq. (3) can be chosen as the averages of those of the two materials: e.g.,  $\mu = (\mu_\alpha + \mu_\beta)/2$ ,  $\nu = (\nu_\alpha + \nu_\beta)/2$ . More accurate values can be adopted if necessary.

Note that the energy  $\gamma$  in Eq. (3) is based on densities of dislocations. When all the constituent dislocations on the interface are straight, the obtained vectors  $\mathbf{N}_j$ 's give the exact dislocation structure. When the dislocation network consists of disconnected dislocation segments, e.g., the hexagonal network, our continuum model gives the line directions and densities of these dislocations (line direction  $\mathbf{N}_j/N_j$  and density  $N_j$ ); and in this case, we will present a method to recover the exact hexagonal network from the obtained dislocation densities and line directions; see the end of this section.

The constraint of the Frank-Bilby formula in Eq. (4) holds for any probe vector  $\mathbf{p}$  if and only if it holds for the two basis vectors of the  $xy$  plane:  $\mathbf{p} = \mathbf{p}_1 = (1, 0)$  and  $\mathbf{p} = \mathbf{p}_2 = (0, 1)$ , i.e.,  $\tilde{\mathbf{h}} = (\mathbf{h}_1, \mathbf{h}_2)^T = \mathbf{0}$  with  $\mathbf{h}_1$  and  $\mathbf{h}_2$  being the Frank-Bilby formula in Eq. (4) when the probe vector  $\mathbf{p}$  is set to be  $\mathbf{p}_1$  and  $\mathbf{p}_2$ , respectively.

In addition to the misfit, the Frank-Bilby equation in Eq. (4) may also include further twist and/or tilt of the two crystals  $\alpha$  and  $\beta$  through the transformation matrices  $\mathbf{S}_\alpha$  and  $\mathbf{S}_\beta$  [6, 7, 8, 9, 10, 11, 12, 13]. When there are rotations around an axis perpendicular to the interface (i.e., twist), assuming that the rotation angles of the natural lattices of the two materials and the reference lattice are  $\theta_\alpha$ ,  $\theta_\beta$  and  $\theta$ , respectively, the Burgers vectors in the rotated reference lattice can be calculated using the rotation matrix  $\mathbf{R}_\theta$  as  $\mathbf{b}_i^R = \mathbf{R}_\theta \mathbf{b}_i$ , and the distortion transformation matrices are  $\mathbf{S}_\alpha^R = \mathbf{R}_\theta \mathbf{S}_\alpha \mathbf{R}_\theta^T$  and  $\mathbf{S}_\beta^R = \mathbf{R}_\theta \mathbf{S}_\beta \mathbf{R}_\theta^T$ , where  $\mathbf{b}_i$ ,  $\mathbf{S}_\alpha$  and  $\mathbf{S}_\beta$  are those in the un-rotated state.

**Remarks:**

1. The interface energy formula in Eq. (3) can also be generalized to include elastic anisotropy based on the energy of straight dislocations with appropriate pre-logarithmic energy coefficients [20].

2. We adopt the local energy of the constituent dislocations of the interface for a simple form and efficient calculation of the continuum model. In principle, the local energy in Eq. (3) can be replaced by the full elastic energy with elastic anisotropy and/or different

elastic constants in the two materials [22, 8, 10, 11, 12, 13] for more accurate results.

Numerically, the constrained minimization problem can be solved by the penalty method [23], in which it is approximated by the following **unconstrained minimization problem**:

$$\text{minimize } Q = \int_S \left( \gamma + \frac{\alpha_p}{2} \|\tilde{\mathbf{h}}\|^2 \right) dS, \quad (5)$$

where  $\alpha_p > 0$  with large value is the penalty parameter. It has been shown that as the penalty parameter  $\alpha_p \rightarrow +\infty$ , the solution of this unconstrained minimization problem converges to the solution of the constrained minimization problem [23]. (Other method such as the augmented Lagrangian method can also be used to solve this constrained minimization problem [23].)

This unconstrained problem is still very challenging to solve due to the nonconvexity of the interface energy. We make a further simplification by considering uniform distributions of straight dislocations on the interface. In this case, each  $\mathbf{N}_j = (N_{jx}, N_{jy})$  is a constant vector, and the problem is reduced to minimize  $q = \gamma + \alpha_p \|\tilde{\mathbf{h}}\|^2/2$ .

This unconstrained problem can be solved by gradient minimization with respect to variables  $N_{jx}, N_{jy}, j = 1, 2, \dots, J$ , which leads to the following evolution equations with an artificial time:

$$(N_{jx})_t = - \left( \frac{\partial \gamma}{\partial N_{jx}} + \alpha_p \frac{\partial c}{\partial N_{jx}} \right), \quad (N_{jy})_t = - \left( \frac{\partial \gamma}{\partial N_{jy}} + \alpha_p \frac{\partial c}{\partial N_{jy}} \right), \quad (6)$$

for  $j = 1, 2, \dots, J$ , where  $c = \|\tilde{\mathbf{h}}\|^2/2$ , and  $\tilde{\mathbf{h}} = (h_1, h_2, h_3, h_4)^T$  with  $h_1 = \sum_{j=1}^J b_{jx} N_{jx} - (\mathbf{S}_\beta^{-1}[1, 1] - \mathbf{S}_\alpha^{-1}[1, 1])$ ,  $h_2 = \sum_{j=1}^J b_{jy} N_{jx} - (\mathbf{S}_\beta^{-1}[2, 1] - \mathbf{S}_\alpha^{-1}[2, 1])$ ,  $h_3 = \sum_{j=1}^J b_{jx} N_{jy} - (\mathbf{S}_\beta^{-1}[1, 2] - \mathbf{S}_\alpha^{-1}[1, 2])$ ,  $h_4 = \sum_{j=1}^J b_{jy} N_{jy} - (\mathbf{S}_\beta^{-1}[2, 2] - \mathbf{S}_\alpha^{-1}[2, 2])$ . Note that when tilt of the two crystals  $\alpha$  and  $\beta$  is also considered, in the Frank-Bilby equation in Eq. (4),  $\mathbf{S}_\alpha$  and  $\mathbf{S}_\beta$  will be  $3 \times 3$  matrices,  $\mathbf{b}_j, \mathbf{p}$  and  $\mathbf{h}$  will be vectors in three dimensions, and  $\tilde{\mathbf{h}}$  will be a  $6 \times 1$  vector.

**Identification of dislocation structure from dislocation densities.** Now we present a method that recovers the exact dislocation structure based on the densities and orientations of the constituent dislocations obtained in our continuum model. As mentioned



above, when all the constituent dislocations on the interface are straight, the obtained vectors  $\mathbf{N}_j$ 's give the exact dislocation structure directly. In a general dislocation structure, due to dislocation reactions, the dislocations may not necessarily be continuous straight lines, and they may form hexagons (not necessarily regular) with disconnected dislocation segments; see Fig. 5(b) for an example. In the identification method, we calculate the exact length and orientation of each dislocation segment in the hexagonal network based on the dislocation densities and orientations obtained by the continuum model.

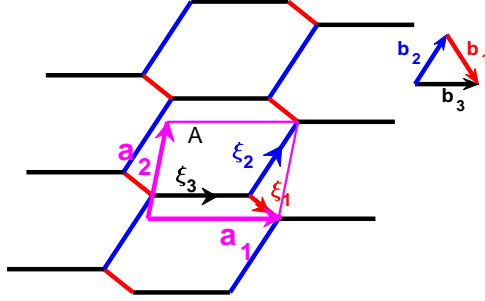


Figure 2: A hexagonal dislocation structure that consists of dislocations with Burgers vectors  $\mathbf{b}_1$ ,  $\mathbf{b}_2$  and  $\mathbf{b}_3$ , whose line directions are  $\xi_1$ ,  $\xi_2$ , and  $\xi_3$ , respectively. Vectors  $\mathbf{a}_1$  and  $\mathbf{a}_2$  are the two sides of the periodic parallelogram unit cell. The area of a unit cell is  $A = \|\mathbf{a}_1 \times \mathbf{a}_2\|$ .

Consider a hexagonal network with dislocations of three Burgers vectors  $\mathbf{b}_1$ ,  $\mathbf{b}_2$ , and  $\mathbf{b}_3$ , in which dislocations may have reactions, e.g,  $\mathbf{b}_3 = \mathbf{b}_1 + \mathbf{b}_2$  and  $b_2^2 < b_1^2 + b_2^2$ ; see Fig. 2. In this hexagonal network, as we discussed before, the direction of dislocation generated by  $\mathbf{b}_j$  is  $\xi_j = (\mathbf{N}_j/N_j) \times \mathbf{n}$ , and the density of these dislocations is  $N_j$ . Consider a periodic parallelogram cell as shown in Fig. 2. It can be calculated that the  $\mathbf{b}_1$ -,  $\mathbf{b}_2$ -, and  $\mathbf{b}_3$ -dislocation segments in the parallelogram, written in the vector form, are  $\mathbf{l}_1 = AN_1 \times \mathbf{n}$ ,  $\mathbf{l}_2 = AN_2 \times \mathbf{n}$ ,  $\mathbf{l}_3 = AN_3 \times \mathbf{n}$ , respectively, where  $\mathbf{n}$  is the normal vector of the interface, and  $A$  is the area of the periodic parallelogram cell. Using these results, it can be solved that in a periodic parallelogram cell, the length of each dislocation segment is

$$l_j = \frac{N_j}{\|\mathbf{N}_1 \times \mathbf{N}_2\| + \|\mathbf{N}_2 \times \mathbf{N}_3\| + \|\mathbf{N}_3 \times \mathbf{N}_1\|}, \quad j = 1, 2, 3, \quad (7)$$

Using this formula of length of each dislocation segment  $l_j$  and its direction  $\boldsymbol{\xi}_j = (\mathbf{N}_j/N_j) \times \mathbf{n}$ , we can draw the exact hexagonal network structure based on the dislocation densities and orientations represented by  $\{\mathbf{N}_j\}$  in the continuum model.

## 4. Reference lattice and possible Burgers vectors

In this section, we briefly review the reference lattice and possible Burgers vectors for the dislocation network on a semicoherent interface. The distortion transformation matrices  $\mathbf{S}_\alpha$  and  $\mathbf{S}_\beta$  are defined as the matrices mapping from the dichromatic patterns of the two lattices  $\alpha$  and  $\beta$  to the reference lattice, and the possible Burgers vectors are the lattice vectors in the reference lattice [3]. In practice, the median lattice (average of the two lattices) or one of the adjacent lattices have often been used as the reference lattice [16, 21, 3]. Especially, the median lattice [16] is an excellent approximation of the reference lattice for symmetric and isotropic interfaces, leading to equal partition of the elastic fields of the two crystals. Recently, methods of determining the reference lattice in general cases such as anisotropic or unsymmetrical interfaces have also been developed [6, 7, 8, 9, 10, 11].

Figure 3 shows the reference lattices and possible Burgers vectors of several semicoherent interfaces between fcc and bcc lattices that have been studied recently in the literature [6, 7, 8, 9, 10, 11, 12, 13, 14]. In Fig. 3(a), the interface orientation relationships are  $(110)_{\text{fcc}} \parallel (001)_{\text{bcc}}$ ,  $[001]_{\text{fcc}} \parallel [010]_{\text{bcc}}$  (in  $x$ -direction) and  $[1\bar{1}0]_{\text{fcc}} \parallel [100]_{\text{bcc}}$  (in  $y$ -direction). The natural dichromatic patterns of the fcc and bcc lattices are rectangles with parallel sides, as shown by the red and blue dashed lines, respectively, in Fig. 3(a). The coherent dichromatic pattern of the reference lattice is also a rectangle pattern in between the fcc and bcc natural dichromatic patterns, as shown by the black dashed lines in Fig. 3(a). When the median lattice (the average of the fcc and bcc natural dichromatic patterns) is adopted as the reference lattice, the possible Burgers vectors of dislocations on the semicoherent interface

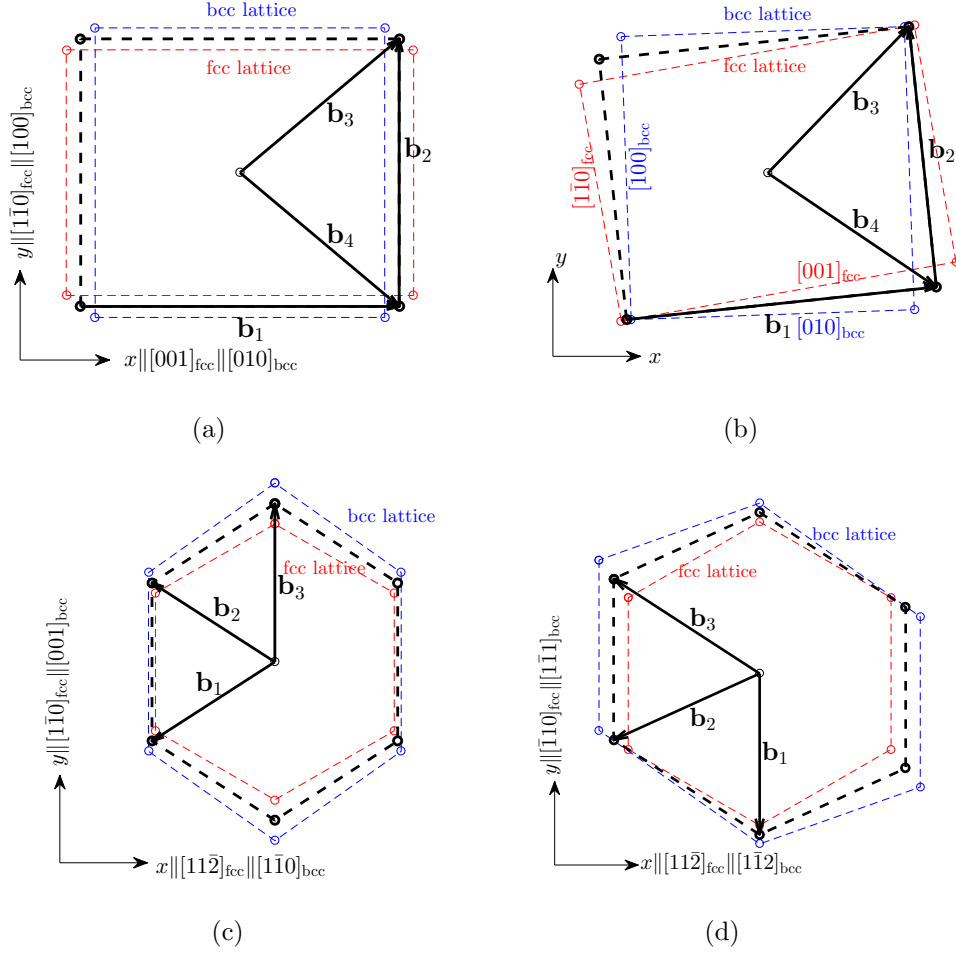


Figure 3: Geometry of the dichromatic patterns, reference states and possible Burgers vectors of some classical semicoherent interfaces between fcc and bcc lattices. The natural dichromatic patterns of the fcc and bcc lattices and the reference lattice (the median lattice) are polygons with red, blue, and black dashed lines, respectively. The possible Burgers vectors defined in the reference lattice are shown by black arrows. (a) Interface with the orientation relationship  $(110)_{\text{fcc}} \parallel (001)_{\text{bcc}}$ ,  $[001]_{\text{fcc}} \parallel [010]_{\text{bcc}}$ , and  $[1\bar{1}0]_{\text{fcc}} \parallel [100]_{\text{bcc}}$ . The natural dichromatic patterns are rectangles. (b) Interface with the orientation relationship of that in (a) with further rotations around an axis perpendicular to the interface. The reference lattice and possible Burgers vectors can all be obtained by rotations from those in (a). (c) Interface with the NW orientation relationship:  $(111)_{\text{fcc}} \parallel (110)_{\text{bcc}}$ ,  $[11\bar{2}]_{\text{fcc}} \parallel [1\bar{1}0]_{\text{bcc}}$ , and  $[1\bar{1}0]_{\text{fcc}} \parallel [001]_{\text{bcc}}$ . The natural dichromatic patterns are hexagons. (d) Interface with the KS orientation relationship:  $(111)_{\text{fcc}} \parallel (110)_{\text{bcc}}$ ,  $[11\bar{2}]_{\text{fcc}} \parallel [1\bar{1}2]_{\text{bcc}}$ , and  $[\bar{1}10]_{\text{fcc}} \parallel [1\bar{1}1]_{\text{bcc}}$ . The fcc and bcc lattices, reference lattice patterns and Burgers vectors can be obtained by rotating the corresponding ones in the NW orientation relationship in (c) around an axis perpendicular to the interface.

are the lattice vectors of the reference lattice:

$$\mathbf{b}_1 = \left( \frac{1}{2}a_{\text{fcc}} + \frac{1}{2}a_{\text{bcc}}, 0 \right), \mathbf{b}_2 = \left( 0, \frac{\sqrt{2}}{4}a_{\text{fcc}} + \frac{1}{2}a_{\text{bcc}} \right),$$

$$\mathbf{b}_3 = \left( \frac{1}{4}a_{\text{fcc}} + \frac{1}{4}a_{\text{bcc}}, \frac{\sqrt{2}}{8}a_{\text{fcc}} + \frac{1}{4}a_{\text{bcc}} \right), \mathbf{b}_4 = \left( \frac{1}{4}a_{\text{fcc}} + \frac{1}{4}a_{\text{bcc}}, - \left( \frac{\sqrt{2}}{8}a_{\text{fcc}} + \frac{1}{4}a_{\text{bcc}} \right) \right), \quad (8)$$

and the distortion transformation matrices mapping from the fcc and bcc lattices to the reference lattice are

$$\mathbf{S}_\alpha = \begin{pmatrix} \frac{a_{\text{fcc}}+a_{\text{bcc}}}{2a_{\text{fcc}}} & 0 \\ 0 & \frac{\frac{\sqrt{2}}{2}a_{\text{fcc}}+a_{\text{bcc}}}{\sqrt{2}a_{\text{fcc}}} \end{pmatrix}, \quad \mathbf{S}_\beta = \begin{pmatrix} \frac{a_{\text{fcc}}+a_{\text{bcc}}}{2a_{\text{bcc}}} & 0 \\ 0 & \frac{\frac{\sqrt{2}}{2}a_{\text{fcc}}+a_{\text{bcc}}}{2a_{\text{bcc}}} \end{pmatrix}, \quad (9)$$

where  $a_{\text{fcc}}$  and  $a_{\text{bcc}}$  are the lattice constants of the fcc and bcc lattices.

Figure 3(b) shows the orientation relationship of the fcc(110)/bcc(001) interface in Fig. 3(a) with further rotations around an axis perpendicular to the interface. The rotation angles of the natural fcc, bcc lattices and the reference lattice are  $\theta_\alpha$ ,  $\theta_\beta$  and  $\theta$ , respectively. The Burgers vectors in the rotated reference lattice can be calculated by multiplying the Burgers vectors in the un-rotated reference lattice by the rotation matrix  $\mathbf{R}_\theta$ , i.e.,

$$\mathbf{b}_i^{\text{R}} = \mathbf{R}_\theta \mathbf{b}_i, \quad \text{with } \mathbf{R}_\theta = \begin{pmatrix} \cos \theta & -\sin \theta \\ \sin \theta & \cos \theta \end{pmatrix}. \quad (10)$$

The distortion transformation matrices are

$$\mathbf{S}_\alpha^{\text{R}} = \mathbf{R}_\theta \mathbf{S}_\alpha \mathbf{R}_\alpha^{\text{T}}, \quad \mathbf{S}_\beta^{\text{R}} = \mathbf{R}_\theta \mathbf{S}_\beta \mathbf{R}_\beta^{\text{T}}. \quad (11)$$

Figure 3(c) demonstrates the classical Nishiyama-Wassermann (NW) orientation relationship:  $(111)_{\text{fcc}} \parallel (110)_{\text{bcc}}$ ,  $[11\bar{2}]_{\text{fcc}} \parallel [1\bar{1}0]_{\text{bcc}}$  (in  $x$ -direction), and  $[1\bar{1}0]_{\text{fcc}} \parallel [001]_{\text{bcc}}$  (in  $y$ -direction). The natural dichromatic patterns of fcc and bcc lattices are hexagonal patterns, and the coherent dichromatic pattern of the reference lattice, which is the median lattice between the fcc and bcc lattices, is also a hexagonal pattern. The possible Burgers vectors defined in the reference lattice are

$$\begin{aligned} \mathbf{b}_1 &= \left( -\left( \frac{\sqrt{6}}{8}a_{\text{fcc}} + \frac{\sqrt{2}}{4}a_{\text{bcc}} \right), -\left( \frac{\sqrt{2}}{8}a_{\text{fcc}} + \frac{1}{4}a_{\text{bcc}} \right) \right), \\ \mathbf{b}_2 &= \left( -\left( \frac{\sqrt{6}}{8}a_{\text{fcc}} + \frac{\sqrt{2}}{4}a_{\text{bcc}} \right), \frac{\sqrt{2}}{8}a_{\text{fcc}} + \frac{1}{4}a_{\text{bcc}} \right), \quad \mathbf{b}_3 = \left( 0, \frac{\sqrt{2}}{4}a_{\text{fcc}} + \frac{1}{2}a_{\text{bcc}} \right), \end{aligned} \quad (12)$$

and the distortion transformation matrices are

$$\mathbf{S}_\alpha = \begin{pmatrix} \frac{\frac{\sqrt{6}}{4}a_{\text{fcc}} + \frac{\sqrt{2}}{2}a_{\text{bcc}}}{\frac{\sqrt{6}}{2}a_{\text{fcc}}} & 0 \\ 0 & \frac{\frac{\sqrt{2}}{2}a_{\text{fcc}} + a_{\text{bcc}}}{\sqrt{2}a_{\text{fcc}}} \end{pmatrix}, \quad \mathbf{S}_\beta = \begin{pmatrix} \frac{\frac{\sqrt{6}}{4}a_{\text{fcc}} + \frac{\sqrt{2}}{2}a_{\text{bcc}}}{\sqrt{2}a_{\text{bcc}}} & 0 \\ 0 & \frac{\frac{\sqrt{2}}{2}a_{\text{fcc}} + a_{\text{bcc}}}{2a_{\text{fcc}}} \end{pmatrix}. \quad (13)$$

Another classical orientation relationship of the interface jointing  $(111)_{\text{fcc}} \parallel (110)_{\text{bcc}}$  is the Kurdjumov-Sachs (KS) orientation relationship with  $[11\bar{2}]_{\text{fcc}} \parallel [1\bar{1}2]_{\text{bcc}}$  (in  $x$ -direction) and  $[\bar{1}10]_{\text{fcc}} \parallel [1\bar{1}1]_{\text{bcc}}$  (in  $y$ -direction); see Fig. 3(d). It can be obtained by rotating the fcc and bcc lattices in NW orientation relationship around an axis perpendicular to the interface. The possible Burgers vectors and the distortion transformation matrices can also be obtained from those in the NW orientation relationship by rotations using Eqs. (10) and (11).

## 5. Numerical simulation

We apply our continuum simulation model to obtain dislocation structures on the semicoherent interfaces of Cu(110)/Nb(001) and Cu(111)/Nb(110), which have been studied recently in the literature [6, 7, 8, 9, 10, 11, 12, 13, 14]. The orientation relationships, reference states (the median lattices) and possible Burgers vectors of these interfaces are shown in Fig. 3. The lattice constants of Cu and Nb are  $a_{\text{Cu}} = 0.360\text{nm}$  and  $a_{\text{Nb}} = 0.330\text{nm}$ , respectively. We start from  $N_{jx} = N_{jy} = 0$ ,  $j = 1, 2, \dots, J$ , when performing the energy gradient minimization in Eq. (6). We choose a large value for the penalty parameter  $\alpha_p$  in Eq. (5) and further increases of its value give only negligible changes in the converged dislocation structures. We compare our results with those obtained using atomistic simulations [7, 9]. The reference lattices of these semicoherent interfaces obtained by atomistic simulations [7, 9] are very close to the median lattices adopted in our simulations.

### 5.1. Cu(110)/Nb(001) interface with rectangle pattern

We first consider the Cu(110)/Nb(001) interface with the orientation relationship as shown in Fig. 3(a), where the natural Cu (fcc), Nb (bcc), and reference lattices have rectangle patterns. There are four possible Burgers vectors  $\mathbf{b}_j$ ,  $j = 1, 2, 3, 4$ . See Eqs. (8) and (9) for the formulas of these Burgers vectors and the distortion matrices  $\mathbf{S}_\alpha$  and  $\mathbf{S}_\beta$ .

The dislocation structure obtained using our continuum model is shown in Fig. 4. The dislocation structure is a rectangular network that consists of two arrays of dislocations with

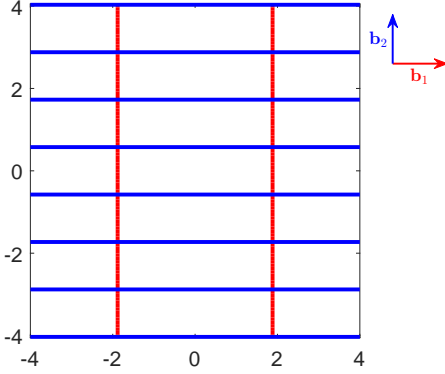


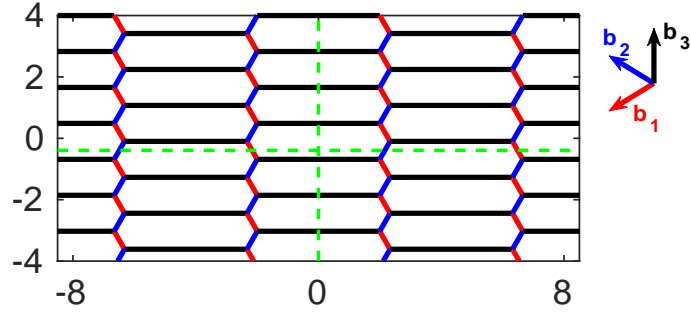
Figure 4: Dislocation structure of this Cu(110)/Nb(001) interface calculated using our continuum model. It is a rectangular network that consists of two arrays of dislocations with Burgers vectors  $\mathbf{b}_1$  and  $\mathbf{b}_2$  (red vertical lines and blue horizontal lines, respectively). Unit: nm.

Burgers vectors  $\mathbf{b}_1$ ,  $\mathbf{b}_2$  and represented by the reciprocal vectors  $\mathbf{N}_1 = (-0.2658, 0)/\text{nm}$ ,  $\mathbf{N}_2 = (0, 0.8681)/\text{nm}$ , respectively. These two arrays of dislocations are both edge dislocations, and are in the  $+y$  ( $[1\bar{1}0]_{\text{Cu}} \parallel [100]_{\text{Nb}}$ ) and  $+x$  ( $[001]_{\text{Cu}} \parallel [010]_{\text{Nb}}$ ) directions, with inter-dislocation distances  $D_1 = 1/N_1 = 3.76\text{nm}$  and  $D_2 = 1/N_2 = 1.15\text{nm}$ , respectively. Dislocations with Burgers vectors  $\mathbf{b}_3$  and  $\mathbf{b}_4$  do not appear in the converged dislocation structure, i.e.,  $\mathbf{N}_3, \mathbf{N}_4$  converge to  $\mathbf{0}$  in the simulation. These results of rectangular network, dislocation line directions and inter-dislocation distances agree excellently with those obtained using atomistic simulation in Ref. [7], in which the inter-dislocation distances in the two dislocation arrays are  $D_1 = 3.80\text{nm}$  and  $D_2 = 1.13\text{nm}$ .

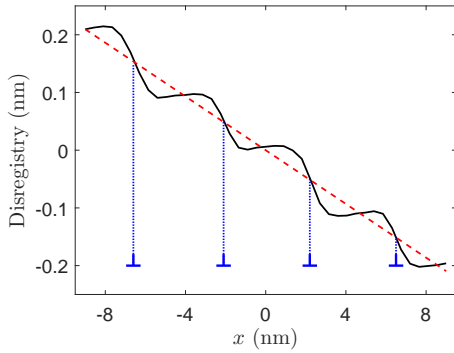
## 5.2. Cu(111)/Nb(110) interface with NW orientation relationship

We then consider the Cu(111)/Nb(110) interface with hexagonal pattern in the classical NW orientation relationship as shown in Fig. 3(c). The natural dichromatic patterns of Cu (fcc) and Nb (bcc) lattices and the coherent dichromatic pattern of the reference lattice are hexagonal patterns. The three possible Burgers vectors defined in the reference lattice and the distortion matrices  $\mathbf{S}_\alpha$  and  $\mathbf{S}_\beta$  are given in Eqs. (12) and (13).

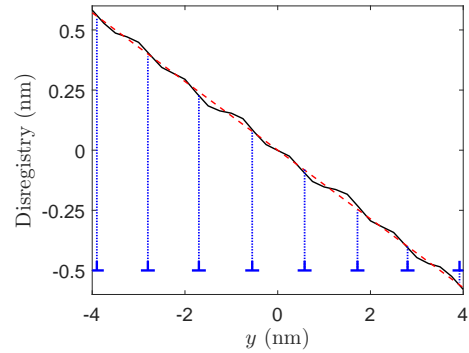
In the dislocation network of this semicoherent interface obtained using our continuum model, dislocations with all the three Burgers vectors are present; see Fig. 5(a). The



(a)



(b)



(c)

Figure 5: (a) Dislocation structure calculated using our continuum model. The dislocation structure consists of a hexagonal network of three arrays of dislocations with Burgers vectors  $\mathbf{b}_1$ ,  $\mathbf{b}_2$  and  $\mathbf{b}_3$ , shown by red, blue and black line segments, respectively. Unit: nm. (b) and (c) Disregistries along some cross-section lines obtained by atomistic simulations in Ref. [9] (reproduced from their data): (b) disregistry in the  $x$  direction ( $[[11\bar{2}]_{\text{Cu}}||[1\bar{1}0]_{\text{Nb}}$ ) along a cross-section line parallel to the  $x$  axis, and (c) disregistry in the  $y$  direction ( $[[1\bar{1}0]_{\text{Cu}}||[001]_{\text{Nb}}$ ) along a cross-section line parallel to the  $y$  axis. The black and red lines show the actual disregistry and the unrelaxed uniform disregistry, respectively. The  $\perp$  symbols show the locations of dislocations.

converged values obtained using our continuum model are  $\mathbf{N}_1 = (-0.1149, -0.0660)/\text{nm}$ ,  $\mathbf{N}_2 = (-0.1149, 0.0660)/\text{nm}$  and  $\mathbf{N}_3 = (0, 0.8022)/\text{nm}$ , respectively. This result means that the dislocations with the three Burgers vectors have line directions of  $\boldsymbol{\xi}_1 = (-0.4981, 0.8671)$ ,  $\boldsymbol{\xi}_2 = (0.4981, 0.8671)$  and  $\boldsymbol{\xi}_3 = (1, 0)$  in the  $xy$  plane, respectively, and their densities are  $\rho_1 = N_1 = 0.1325/\text{nm}$ ,  $\rho_2 = N_2 = 0.1325/\text{nm}$  and  $\rho_3 = N_3 = 0.8022/\text{nm}$ , respectively. Recall that the local dislocation line direction is calculated by  $\boldsymbol{\xi}_j = (\mathbf{N}_j/N_j) \times \mathbf{n}$ , where  $\mathbf{n}$  is the unit normal vector of the interface. The  $\mathbf{b}_3$ -dislocations are edge dislocations, and the  $\mathbf{b}_1$ - and  $\mathbf{b}_2$ -dislocations are very close to edge, with an angle of  $93^\circ$  between the dislocations and their Burgers vectors.

These three arrays of dislocations form a hexagonal network, because we have  $\mathbf{b}_3 = (-\mathbf{b}_1) + \mathbf{b}_2$  with  $b_3^2 < b_1^2 + b_2^2$  and dislocation reaction from a  $\mathbf{b}_1$ -dislocation and a  $\mathbf{b}_2$ -dislocation into a  $\mathbf{b}_3$ -dislocation is energetically favorable. In this case, dislocations are disconnected segments instead of connected straight lines. Using the identification method presented at the end of Sec. 3 (Eq. (7)), we can calculate the lengths of the three types of dislocation segments, which are 0.6642nm, 0.6642nm and 4.0208nm for the  $\mathbf{b}_1$ -,  $\mathbf{b}_2$ -, and  $\mathbf{b}_3$ -dislocation segments, respectively. Based on these orientations and lengths of these dislocation segments, we can recover the hexagonal network as shown in Fig. 5(a).

We compare the dislocation structure obtained by our continuum model with the atomistic simulation result in Ref. [9]. Disregistries along some cross-section lines obtained by atomistic simulations in Ref. [9] are shown in Figs. 5(b) and (c). Figure 5(b) shows the disregistry in the  $x$  direction ( $[11\bar{2}]_{\text{Cu}} \parallel [1\bar{1}0]_{\text{Nb}}$ ) along a cross-section line parallel to the  $x$  axis, and this cross-section line intersects with dislocations periodically with average distance of 4.40nm between two neighboring intersecting points. Figure 5(c) shows the disregistry in the  $y$  direction ( $[1\bar{1}0]_{\text{Cu}} \parallel [001]_{\text{Nb}}$ ) along a cross-section line parallel to the  $y$  axis, and this cross-section line intersects with dislocations periodically with average distance between two neighboring intersecting points 1.14nm. On the other hand, in the dislocation structure obtained by our continuum model shown in Fig. 5(a), the horizontal line intersects with four  $\mathbf{b}_1$ - and  $\mathbf{b}_2$ -dislocations for  $-8\text{nm} \leq x \leq 8\text{nm}$  and the distance between two neighboring intersecting points is 4.35nm, and the vertical line intersects with the array of the



$\mathbf{b}_3$ -dislocation segments with inter-dislocation distance of 1.15nm. These results agree excellently with those of atomistic simulations shown in Figs. 5(b) and (c) (see also Figs. 3-5 in Ref. [9]).

Dislocation structure on the NW semicoherent interface as well as the reference state have also be obtained in Ref. [13] by using their continuum framework, in which a full anisotropic elasticity problem in the bulk of bicrystal is solved and the hexagonal network on the interface with new dislocation segments with the third Burgers vector is formed by dislocation reaction from the lozenge dislocation network of two sets of dislocations. The hexagonal networks obtained by using our continuum model and that by using their model (Fig. 6(d) in Ref. [13]) are quite similar to each other. Quantitatively, across the same horizontal line as that in Fig. 5(a), the distance between two neighboring intersecting points is 4.05nm in their result (measured from their Fig. 6(d)), and the distance between neighboring  $\mathbf{b}_3$ -dislocation segments is 1.13nm (calculated from their data of the lozenge dislocation network). These agreements between the results of the two models provide mutual validations of these models.

### 5.3. Cu(111)/Nb(110) interface with KS orientation relationship

We also consider the Cu(111)/Nb(110) interface with hexagonal pattern in the KS orientation relationship as shown in Fig. 3(d), in which there is a relative rotation between the natural Cu fcc and Nb bcc lattices. The rotation angle of the natural Cu fcc lattice is  $\theta_\alpha = 60^\circ$ , and that of the natural Nb bcc lattice is  $\theta_\beta = 54.74^\circ$ . The rotation angle of the reference lattice is approximately chosen as the average of  $\theta_\alpha$  and  $\theta_\beta$ , i.e.,  $\theta = (\theta_\alpha + \theta_\beta)/2$ . The three possible Burgers vectors and the distortion matrices of this interface can be calculated by rotations from the corresponding ones in the interface with the NW orientation relationship, using Eqs. (10), (11) and (12), (13).

Simulation result using our continuum model shows that the dislocation structure of this Cu(111)/Nb(110) interface with KS orientation relationship consists of a parallelogram network of two arrays of dislocations with Burgers vectors  $\mathbf{b}_1$  and  $\mathbf{b}_3$  represented by the

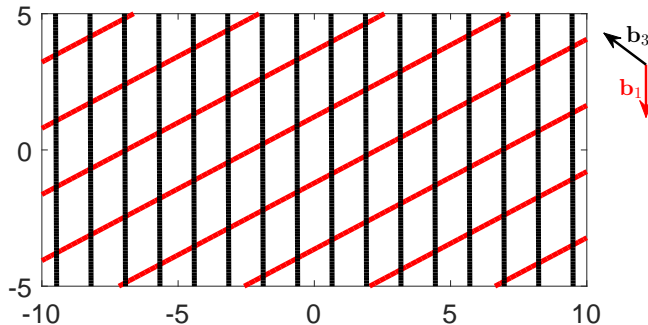


Figure 6: Dislocation structure of the Cu(111)/Nb(110) interface in KS OR calculated using our continuum model. The dislocation structure consists of a parallelogram network of dislocation arrays with Burgers vectors  $\mathbf{b}_1$  and  $\mathbf{b}_3$ , shown by red and black lines, respectively.

reciprocal vectors  $\mathbf{N}_1 = (0.2173, -0.4118)/\text{nm}$  and  $\mathbf{N}_3 = (-0.7913, -0.0032)/\text{nm}$ , respectively; see Fig. 6 for the obtained dislocation network. These results of the continuum model mean that the two arrays of dislocations have line directions  $\boldsymbol{\xi}_1 = (-0.8844, -0.4667)$  and  $\boldsymbol{\xi}_2 = (-0.0040, 1.0000)$  with inter-dislocation distances  $D_1 = 2.148\text{nm}$  and  $D_3 = 1.264\text{nm}$ , respectively. Accordingly, the angles between the two arrays of dislocations and the  $x$  axis are  $-152.2^\circ$  and  $90.2^\circ$ , respectively. We compare this dislocation structure with that obtained by atomistic simulation in Ref. [9] (Figs. 8 and 9 in Ref. [9]), and observe excellent agreement between the two results. In the atomistic simulation result in Ref. [9], the inter-dislocation distances in the two arrays of dislocations are  $D_1 = 2.131\text{nm}$ ,  $D_3 = 1.245\text{nm}$  and the dislocation line directions have angles  $152^\circ$  and  $90^\circ$  with respect to the  $x$ -axis, respectively (see Table 2 in Ref. [9]. Notice that the  $+z$  direction is pointing downward there).

## 6. Conclusions

In summary, we have developed a continuum model for the dislocation structures of semicoherent interfaces based on constrained energy minimization. In our model, the dislocation structure of a semicoherent interface is obtained by minimizing the energy of the equilibrium dislocation network with respect to all the possible Burgers vectors, subject to the constraint of the Frank-Bilby equation. Comparisons with atomistic simulation results and results of

other available models show that our continuum model is able to give excellent predictions of dislocation structures on semicoherent interfaces.

## Acknowledgements

This work was supported by the Hong Kong Research Grants Council General Research Fund through grant 16302818.

## Data availability

The datasets generated in study are available upon request.

## References

## References

- [1] J. H. van der Merwe, On the stresses and energies associated with intercrystalline boundaries, *Proc. Phys. Soc. London A* 63 (1950) 616–637.
- [2] J. M. Matthews, Accommodation of misfit across the interface between singlecrystal films of various face-centred cubic metals, *Philos. Mag.* 13 (1966) 1207–1221.
- [3] A. P. Sutton, R. W. Balluffi, *Interfaces in Crystalline Materials*, Clarendon Press, Oxford, 1995.
- [4] S. S. Quek, Y. Xiang, D. J. Srolovitz, Loss of interface coherency around a misfitting spherical inclusion, *Acta Mater.* 59 (2011) 5398–5410.
- [5] R. Shi, N. Ma, Y. Wang, Predicting equilibrium shape of precipitates as function of coherency state, *Acta Mater.* 60 (2012) 4172–4184.
- [6] J. P. Hirth, R. C. Pond, R. G. Hoagland, X. Y. Liu, J. Wang, Interface defects, reference spaces and the Frank-Bilby equation, *Prog. Mater. Sci.* 58 (2013) 749–823.
- [7] J. Wang, R. Zhang, C. Zhou, I. J. Beyerlein, A. Misra, Characterizing interface dislocations by atomically informed frank-bilby theory, *J. Mater. Res.* 28 (13) (2013) 1646–1657.
- [8] A. J. Vattre, M. J. Demkowicz, Determining the burgers vectors and elastic strain energies of interface dislocation arrays using anisotropic elasticity theory, *Acta Mater.* 61 (2013) 5172–5187.

- [9] J. Wang, R. Zhang, C. Zhou, I. Beyerlein, A. Misra, Interface dislocation patterns and dislocation nucleation in face-centered-cubic and body-centered-cubic bicrystal interfaces, *Int. J. Plast.* 53 (2014) 40–55.
- [10] A. Vattre, M. Demkowicz, Partitioning of elastic distortions at a semicoherent heterophase interface between anisotropic crystals, *Acta Mater.* 82 (2015) 234–243.
- [11] N. Abdolrahim, M. J. Demkowicz, Determining coherent reference states of general semicoherent interfaces, *Comput. Mater. Sci.* 118 (2016) 297–308.
- [12] A. Vattre, Elastic strain relaxation in interfacial dislocation patterns: I. a parametric energy-based framework, *J. Mech. Phys. Solids* 105 (2017) 254–282.
- [13] A. Vattre, E. Pan, Three-dimensional interaction and movements of various dislocations in anisotropic bicrystals with semicoherent interfaces, *J. Mech. Phys. Solids* 116 (2018) 185–216.
- [14] S. Shao, F. Akasheh, J. Wang, Y. Liu, Alternative misfit dislocations pattern in semi-coherent fcc {100} interfaces, *Acta Mater.* 114 (2018) 177–186.
- [15] E. Y. Chen, R. Dingreville, C. Deo, Misfit dislocation networks in semi-coherent miscible phase boundaries: An example for U-Zr interfaces, *Comput. Mater. Sci.* 154 (2018) 194–203.
- [16] F. C. Frank, The resultant content of dislocations in an arbitrary intercrystalline boundary, *Symposium on the Plastic Deformation of Crystalline Solids* (1950) 150–154.
- [17] B. A. Bilby, Bristol conference report on defects in crystalline materials, *Phys. Soc., London* (1955) 123.
- [18] X. Zhu, Y. Xiang, Continuum framework for dislocation structure, energy and dynamics of dislocation arrays and low angle grain boundaries, *J. Mech. Phys. Solids* 69 (2014) 175–194.
- [19] L. Zhang, Y. Gu, Y. Xiang, Energy of low angle grain boundaries based on continuum dislocation structure, *Acta Mater.* 126 (2017) 11–24.
- [20] J. P. Hirth, J. Lothe, *Theory of Dislocations*, 2nd Edition, Wiley, New York, 1982.
- [21] K. M. Knowles, The dislocation geometry of interphase boundaries, *Philos. Mag. A* 46 (1982) 951–969.
- [22] L. E. Shilkrot, D. J. Srolovitz, Elastic analysis of finite stiffness bimaterial interfaces: application to dislocation-interface interactions, *Acta Mater.* 46 (1998) 3063–3075.
- [23] E. K. P. Chong, S. H. Zak, *An Introduction to Optimization*, 4th Edition, Wiley, Hoboken, 2013.